



## Research paper

# Hydration effects on the photoionization energy of 2'-deoxyguanosine 5'-phosphate and activation barriers for guanine methylation by carcinogenic methane diazonium ions



Daniel R. Eichler, Haley A. Hamann, Katherine A. Harte, George A. Papadantonakis\*

Department of Chemistry, University of Illinois at Chicago, 845 W. Taylor St., Room 4500 SES, Chicago, IL 60607, United States

## ARTICLE INFO

## Article history:

Received 28 February 2017

In final form 9 May 2017

Available online 11 May 2017

## ABSTRACT

Results from DFT calculations indicate that states originating from gas-phase ionization of the phosphate and the base are degenerate in *syn*-5'-dGMP<sup>-</sup> and that bulk hydration lowers the base-localized ionization energy by <0.5 eV. Local ionization maps show that micro-hydration leads to the formation of donor and acceptor hydrogen bonds and the ionization energy decreases or increases in each case respectively. The S<sub>N</sub>2 transition states of the methylation reactions of guanine with methane diazonium ions are lower at the N7 than at the O<sup>6</sup> sites and they are influenced by local ionization energy and steric interference.

© 2017 Elsevier B.V. All rights reserved.

## 1. Introduction

The ionization energies of DNA nucleotides and their components provide a quantitative measurement of their electron-donating properties. Electron donation by nucleotides are the key initial steps than can lead to direct DNA damage and mutation [1–4]. It has been established throughout many theoretical and experimental studies that guanine is the most easily damaged DNA base by ionizing UV radiation [5–8] and that the guanine holes created during photoionization [9] are the targets for carcinogenesis [10]. The gas-phase vertical ionization potential (IP) of isolated guanine was measured employing gas-phase He(I) UV photoelectron spectroscopy [11]. However, conditions for a typical He (I) UV photoelectron experiment do not allow the direct measurement of IP for intact nucleotides.

In a recent experimental investigation on the gas-phase vertical and adiabatic ionization potentials, (IP), of 5'-dGMP<sup>-</sup>, employing UV photo-detachment photoelectron spectroscopy, it was reported that the highest occupied molecular orbital (HOMO) resides on the phosphate in the *anti*-5'-dGMP<sup>-</sup> conformation and on the base in the *syn*-5'-dGMP<sup>-</sup> conformation. Further, the base-localized vertical IP was measured as 5.05 ± 0.10 eV and at DFT/B3LYP level of theory was calculated to be 4.90 eV [12].

Water and counterion interactions are among the most important that DNA encounters in biological environments. Such interactions also affect how DNA is impacted by low-energy electrons (0–30 eV) [13]. Therefore, it is important to know more

about these interactions affect the nucleotide IP if we are to better understand DNA damage [8,14,15].

In an experimental investigation of the effects of micro-hydration on the IP of nucleobases employing single photon ionization with tunable vacuum-ultraviolet synchrotron radiation, it was reported that the gas-phase adiabatic, IP<sub>ad</sub> value, extracted from the appearance energy curves, for the guanine monomer is 8.1 ± 0.1 eV. It remains the same (8.0 ± 0.1 eV) for mono-, di- and tri-hydrated guanine [16]. The appearance energies decrease slightly with the addition of water molecules but do not converge to the values reported in the literature for UV ionization of DNA in aqueous solutions [5,7].

DNA bases can be methylated. Methylation of DNA bases is an epigenetic mechanism that occurs by the covalent addition of a methyl group to a base and this has been found to influence a variety of processes including DNA integrity and function. Methylation might also play a role in the onset or course of cancer [17,18].

Guanine in double- or single-stranded DNA can be methylated by carcinogenic agents. One such agent is *N*-methyl-*N*-nitrosourea (MeNU) which can react at the ring nitrogen atoms and exocyclic oxygen atoms via S<sub>N</sub>2 reactions [19] whose reactive intermediates are the methane diazonium ions (MeN<sub>2</sub><sup>+</sup>) formed from nitrosamines via metabolic activation [20]. The carcinogenic activity of MeN<sub>2</sub><sup>+</sup> ions can be attributed to O<sup>6</sup> methylation and N7 methylation through the principal DNA reaction pathway [19]. Ultimately, N7 methylation changes the hydrogen-bonding patterns of guanine in duplex DNA by promoting the formation of an enol tautomeric form of guanine that is equivalent to adenine [21].

In older theoretical studies it was reported that the N7 site of guanine is the most reactive in S<sub>N</sub>2 reactions [14,22–24]. In a more

\* Corresponding author.

E-mail address: [gpapad3@uic.edu](mailto:gpapad3@uic.edu) (G.A. Papadantonakis).

recent theoretical investigation for DNA alkylation activation barriers it was reported that the characterization of the relative reactivity of different sites requires consideration of solvation to describe the interactions of the guanine-methane system with explicit water molecules [25].

The ionization energy of guanine in various sequences is inherently important to the ionization of DNA as well as charge transport [26–28]. In a molecular dynamics simulations study it was reported that hydrated electrons formed upon photoionization can reduce guanine only when a water molecule forms a hydrogen bond to the  $O^6$  site to stabilize the resulting radical anion [29].

The main goal of the present systematic theoretical investigation is to integrate methylation and ionization studies of guanine mononucleotides and its components by probing factors that influence the aqueous photoionization energy (IE) values and barriers for guanine methylation reactions with methane diazonium ions employing DFT and the SM8 Universal Solvation Model [30] utilizing feedback from the local ionization potential maps.

## 2. Methods

All calculations were performed using the Spartan '14 Parallel Suite [31] for Microsoft Windows 7, Professional 64-bit edition on an Intel Xeon E3-1240 v3 processor utilizing 32 GB of RAM. Standard geometries of nucleotide systems in the double-stranded B-DNA conformation were generated using the Molecule Builder of Spartan '14 and were fully optimized employing the Density Functional Theory using the hybrid B3LYP exchange correlation functional with the 6-31+G\* basis set.

Gas-phase vertical ionization potentials were evaluated and reported without zero-point energy (ZPE) corrections. These corrections are very small ( $\sim 0.03$  eV), and are consistent with another investigation employing B3LYP/6-31G(d,p) level of theory [15]. Vertical IPs were used because of the high accuracy with which they can be measured experimentally for comparison to theoretically obtained values.

Aqueous photoionization energy calculations were performed employing the SM8 Universal Solvation Model embedded in the Spartan '14 package. The SM8 Model employs the Generalized Born (GB) approximation for bulk electrostatics and represents the solute molecule as a collection of partial atomic charges in a cavity [30].

The aqueous photoionization energy,  $\Delta G_{aq}$ , is the Gibbs free energy associated with the aqueous ionization energy from the closed-shell ground state molecule to an open-shell radical and it was determined using Eq. (1).

$$\Delta G_{aq} = IP + \Delta \Delta G_{hyd} + V_o \quad (1)$$

In Eq. (1),  $IP$  is the gas-phase vertical ionization potential associated with the removal of an electron from the highest occupied molecular orbital (HOMO),  $V_o$  is the hydrated electron stabilization energy, ( $-1.3$  eV) [32,33] and  $\Delta \Delta G_{hyd}$  is determined by Eq. (2).

$$\Delta \Delta G_{hyd} = \Delta G_{hyd}(r) - \Delta G_{hyd}(n) \quad (2)$$

In Eq. (2),  $\Delta G_{hyd}(n)$  is the Gibbs free energy of hydration before ionization and  $\Delta G_{hyd}(r)$  is the energy after ionization. The entropy contribution in the gas-phase is considered negligible based on the observation that  $T\Delta S$  for the ionization of a hydrogen atom at room temperature is 0.05 eV utilizing electron convention Fermi–Dirac statistics [34].

Local ionization potential maps were computed using the embedded module in Spartan '14 and the  $S_N2$  transition states of the methylation reaction of guanine with methane diazonium ion were examined in the gas- and aqueous- phases at the N7 and  $O^6$  sites of guanine employing the B3LYP/6-31+G\* DFT level of theory

and the SM8 Universal Solvation Model. Transition states were monitored by employing the Energy Profile module as embedded in Spartan '14.

## 3. Results and discussion

### 3.1. Aqueous photoionization threshold energy of 5'-dGMP<sup>-</sup> and its components – hydration in bulk

Table 1 lists results for the gas-phase vertical IPs and aqueous photoionization energies (IEs) for 5'-dGMP<sup>-</sup> and its components. Three different conformations of 5'-dGMP<sup>-</sup> structures are shown in Fig. 1; the anti-conformation, and two *syn*-conformations, *Conf-a*, and *Conf-b*. In *syn-Conf-a*, the oxygen substituent in C2' lies in a sterically hindered position above the furanose ring and the torsion angle about the N-glycosylic bond is 61.30°. An intramolecular hydrogen bond with length 1.849 Å is formed between the hydrogen of the N2 amino group of the purine with the O3 of the phosphate. In *Conf-b* the torsion angle is 70.00° and the intramolecular hydrogen bond between the hydrogen of the N2 amino group of the purine with the O2 of the phosphate is 1.718 Å in length. In the anti-conformation, this steric interference is avoided and the torsion angle is  $-95.30^\circ$ . The *syn-Conf-a* structure is 7.57 kcal mol<sup>-1</sup> and the *syn-Conf-b* is 7.30 kcal mol<sup>-1</sup> lower in energy compared to the *anti*, respectively.

The results indicate that the  $\pi$  HOMO is localized on the phosphate group for the *anti*- and for the *syn-Conf-a* the  $\pi$  HOMO is degenerate with ionizing states originating on the base and the phosphate; its vertical IP is 5.03 eV. This value is in agreement with the value obtained (5.01 eV) employing the partial third order (P3) self-energy approximation method [35]. The vertical IP of *syn-Conf-b* is 4.67 eV with the  $\pi$  HOMO localized on the base and it is very low because more electron density is donated to the aromatic ring as shown in the local ionization map Fig. 1(c) resulting in a lower local IP at N7 as listed in Table 1. The IP value of *Conf-a* (5.03 eV) is in agreement with the vertical electron-detachment energy (5.01 eV), obtained for a similar conformation (sConf2) employing the multiconfigurational second-order perturbation (CASPT2) method at the MP2/cc-pVDZ level optimized ground-state most stable conformer [36] and in full agreement with the experimental value of  $(5.05 \pm 0.10)$  eV [12].

More recently the gas-phase  $IP_{ad}$  of 5'-dGMP<sup>-</sup> was reported as  $4.65 \pm 0.15$  eV, localized on the base employing resonance-enhanced two-photon detachment spectroscopy (R2PD) [37]. This experimental value agrees with the theoretically obtained value of 4.64 eV in the present study. The value of adiabatic  $IP_{ad}$  is lower than the vertical IP because the vertical IP only considers the modification of the charge distribution while the adiabatic IP accounts for the relaxation of the ionized potential energy surface, which needs a finite time to occur.

The calculated value of the *Conf-a syn-5'-dGMP<sup>-</sup>* aqueous IE is 4.61 eV, which is 0.42 eV lower relative to the gas-phase and the ionized state is localized on the base. It is also noteworthy that the same value for the IE results for the *Conf-b*, even though its gas-phase IP is lowered by 0.64 eV. This is clearly an indication that the gas phase ionization energies are very sensitive to the geometry of the molecule while explicit solvent effects eliminate this dependency. This agrees with the key finding that the aqueous medium is efficient in screening the interactions within DNA that occur in gas-phase ionization [8]. The calculated IE value (4.61 eV) for *Conf-a syn-5'-dGMP<sup>-</sup>* agrees with the report that in 266-nm (4.66 eV), ns-pulsed laser photolysis experiments a monophotonic observation of 5'-dGMP<sup>-</sup> was observed [38–40]. Bulk hydration of the *anti*- conformation yields a value of 4.78 eV that prohibits a monophotonic 266-nm ionization.

**Table 1**

Calculated gas- and aqueous-phase vertical ionization energies of 5'-dGMP<sup>-</sup> nucleotide and its components using the DFT B3LYP/6-31+G<sup>\*</sup> Method and the SM8 Universal Solvation Model.

Molecule	IP <sub>ver</sub> (eV)	IE <sub>ver</sub> (eV)	IP <sub>ver</sub> Experimental (eV)	IP <sub>ver</sub> (eV) N7 sites	Notes
G	7.99	4.68	8.28 [11]	8.42	
Anti-dG	7.61	4.69	4.77 ± 0.27 (aq) [43]	8.12	
Syn-dG <sup>***</sup>	7.97	4.83		8.49	
Anti-5'-dGMP <sup>-</sup>	4.90 <sup>*</sup>	4.78 <sup>**</sup>		5.55	
Syn-5'-dGMP <sup>-</sup>	5.03 <sup>**</sup>	4.61	5.05 ± 0.10 [12]	6.20	Conf-a
Syn-5'-dGMP <sup>-</sup>	4.67 <sup>**</sup>	4.61		5.83	Conf-b
9-MeG	7.84	4.69	8.02 [11]	8.31	

<sup>\*</sup> Phosphate ionization.

<sup>\*\*</sup> Base ionization.

<sup>\*\*\*</sup> Hydrogen bond at 5'OH and N3.

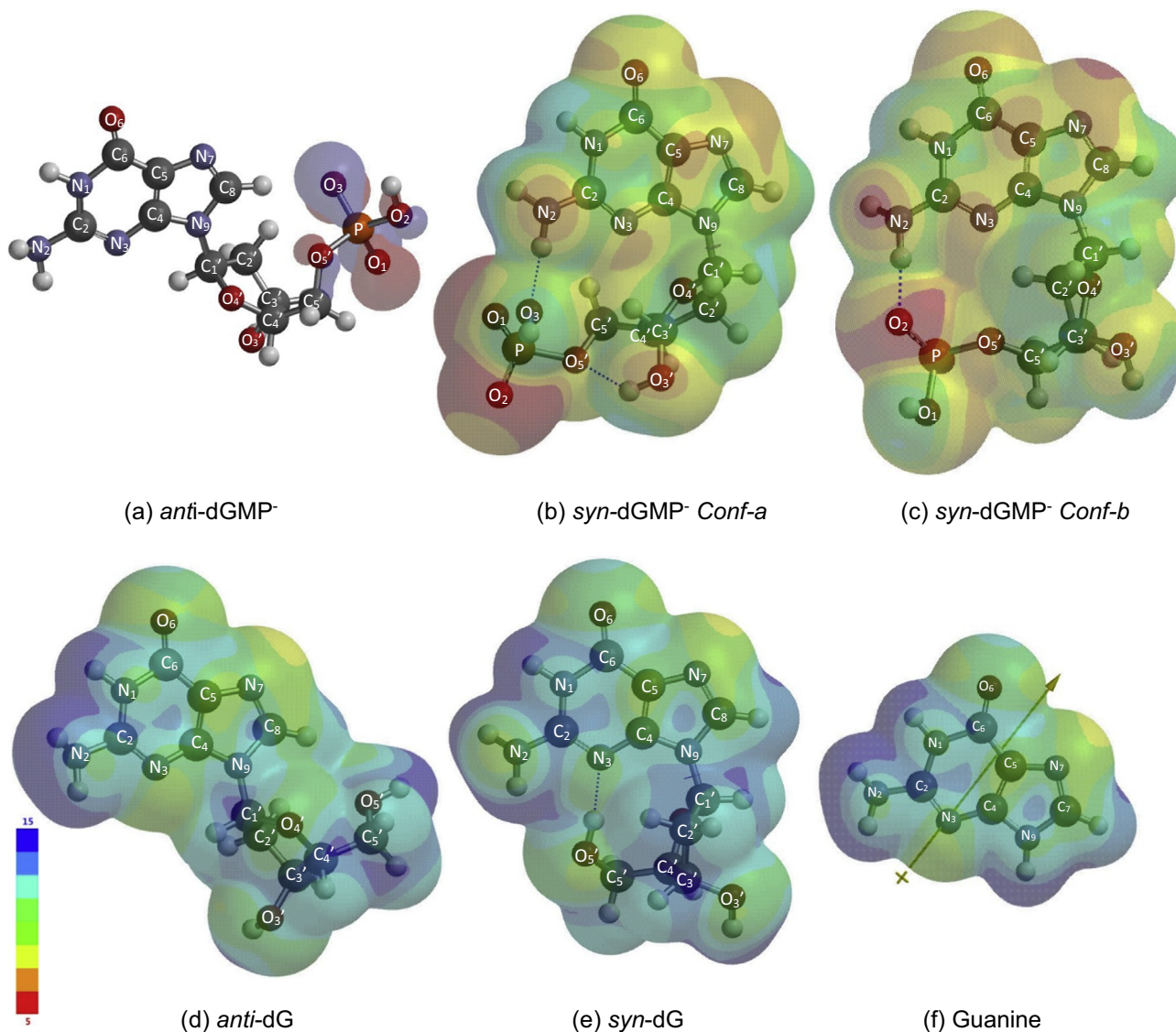


**Fig. 1.** (a) The highest occupied molecular orbital (HOMO) of gas-phase 5' dGMP<sup>-</sup> shows that the electron density is localized on the phosphate moiety in the *anti*-dGMP<sup>-</sup> conformation and ionization is observed at the phosphate. (b) Local ionization map shows that *syn*-5' dGMP<sup>-</sup>-*Conf-a* has less electron density at the N7 site and a higher IP (6.20 eV) compared to the (c) *syn*-5' dGMP<sup>-</sup>-*Conf-b* which has a smaller local IP (5.83 eV) at N7. The distance between the phosphate group and the N2 atom of the amino group in *Conf-b* is shorter and more electron density is pushed toward the guanine ring which results in amino group to becoming a hydrogen donor. This hydrogen donating/accepting property is observed in dG as well. The *anti*-dG molecule, (d), has a local IP at N7 of 8.12 eV, which is lower than the local IP of *syn*-dG (e) (8.49 eV). Unlike *syn*-dGMP<sup>-</sup> where N2 is donating a hydrogen, in *syn*-dG the N3 is accepting a hydrogen and this results in electron density being pulled away from the ring with a consequent increase of the IP. (f) The local ionization map of guanine is shown and the local IP at O<sup>6</sup> is 9.13 eV and at N7 is 8.42 eV indicating that there is more electron density at N7. The legend in the lower left corner correlates to the local ionization potential values on the molecules, where blue shows high IP values and red, orange, and yellow show low IP values.

It can be deduced from Table 1 that the addition of a sugar to guanine lowers the gas-phase vertical IP only modestly, by 0.38 eV in the *anti*-2' deoxyguanosine, dG. The *syn*-dG conformation involves a hydrogen bond between the hydrogen at the N3 atom of the amino group in the purine and the 5'OH of the furanose ring. The calculated IP is 7.97 eV, which is in agreement with values reported in a theoretical investigation of redox potentials [27]. The *anti*-dG conformation is more stable than the *syn*-dG by 5.029 kcal mol<sup>-1</sup>, in agreement with calculations employing the DFT/B3LYP/6-31G\* [41] and the MP2/6-31G\* [42] methods. The calculated IE value for *anti*-dG is 4.69 eV, which is in agreement with the experimentally obtained value of 4.77 ± 0.27 eV [43].

The calculated vertical IP for guanine is 7.99 eV and the experimental value (8.28 eV) refers to canonical N9 – H guanine [11]. Results show that the monobasic phosphate group is responsible for lowering the gas-phase vertical IP of guanine by ~3.0 eV, in agreement with the experimental finding that the charged backbone reduces the gas-phase adiabatic IP for all four nucleotides by ~3.0 eV compared to isolated nucleobases [37]. The experimental IP value for 9-methylguanine (9-MeG) is 8.02 eV [11] and the calculated IP is 7.84 eV, which is in proximity to the value of 7.77 eV obtained employing the OVG-MP2/6-311G (d,p) method [7]. The calculated IE value for 9-MeG is 4.69 eV, almost the same as for free G. 9-MeG is frequently used as a model compound to mimic the glycosidic bond [7,44,45]. Finally, Fig. 1(f) shows the local ionization map of guanine where more electron density is accumulated in the N7 atom lowering the local IP value than at the O<sup>6</sup>. This makes N7 more susceptible to electrophilic attack.

In a recent experimental and theoretical investigation of the oxidation half-reaction of nucleosides and nucleotides in aqueous media the issue of solvent reorganization was addressed [28].

The reorganization energy is the energy needed for the system structure to relax from the neutral ground state structure to the radical cation state and it involves the contribution from the solute and the solvent. It was reported that the solvent contribution is 1.1 eV, the same for all DNA bases. The total reorganization energy for guanosine (GMP) is computed to be 1.5 eV employing the NEPCM for vertical and the PCM for adiabatic models for ionization energies [28]. This reorganization energy value provides an initiative for further investigation of the role of the hydrated electron stabilization energy (–1.3 eV) to the overall reorganization energy.

### 3.2. Micro-hydration of guanine

Fig. 2 shows the positions of the water molecules with respect to guanine in model structures that were used to probe the effect of different hydrogen bonding on the vertical IP of micro-hydrated guanine utilizing the computed local ionization potential maps which provide an indicator of electrophilicity. In the local ionization maps hydrogen bonds are represented by the blue dotted lines and atoms are labeled accordingly. Areas with color towards blue depict areas with less electron density and green-yellowish areas have higher electron density. Table 2 summarizes the changes in gas-phase IP of the micro-hydrated guanine model structures, the location of the hydrogen bonds, their dipole moments, and the local ionization energies at the N7 and O<sup>6</sup> atoms that are implicated in carcinogenesis. The local IPs at N7 are lower than at O<sup>6</sup>.

The local ionization potential maps of guanine tri-hydrated molecules (a–d) are shown in the upper row, the di-hydrated (f–i) in the lower row and the mono-hydrated (e and j) are shown vertically at the right hand side of Fig. 2. In the mono-hydrated

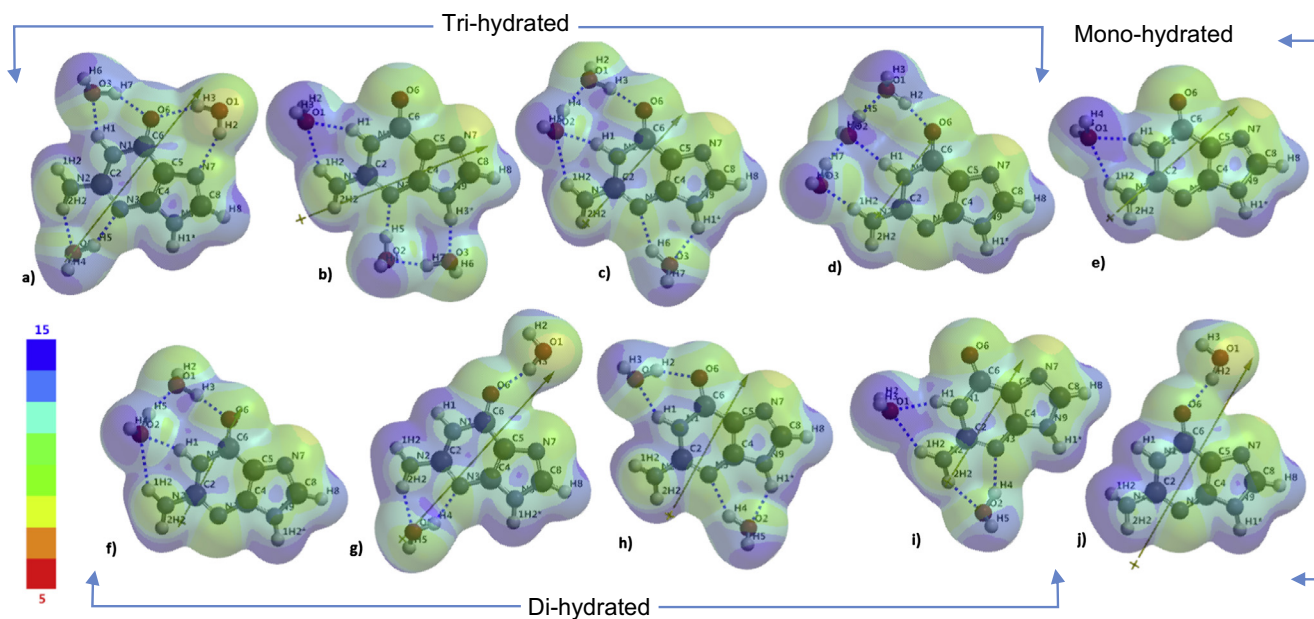


**Fig. 2.** Local ionization potential maps of guanine tri-hydrated (a–d), di-hydrated (f–i), and mono-hydrated molecules (e and j). Blue areas correspond to areas with less electron density and green-yellowish areas correspond to areas with high electron density, concentrated at the N7 and O<sup>6</sup> sites. Blue dotted lines show the hydrogen bonds and the yellow vector lines show the direction and intensity of the dipole moments. The effects of hydrogen bond acceptors and donors as seen in Fig. 1, plays a predominate role with micro-hydration as seen in Fig. 2. As seen in molecules (a–j), the corresponding donor/acceptor ratios are as follows, in (a) 2:4, (b) 3:1, (c) 3:2, (d) 2:1, (e) 2:0, (f) 2:1, (g) 1:2, (h) 2:2, (i) 3:1, and (j) 0:1. When the number of hydrogen acceptors are higher than donors, as seen in molecules (a), (j), and (g), then IPs are higher than the IP of guanine; and when donors are higher than acceptors as seen in molecules (b), (c), (d), (e), (f) and (i) then IPs are lower than the IP of guanine. Small changes also have an effect, which is observable when comparing molecules (b) and (c). When the acceptor was increased by 1 hydrogen bond, the IP increased from 7.64 eV to 7.93 eV. The same is observed when comparing molecules (d), (g), and (h). Molecule (h) has a 2:2 ratio with an IP of 8.01 eV, which is close in value to the IP of guanine 7.99 eV. When a hydrogen donor is reduced by 1 as seen in molecule (g), then the IP increases to 8.20 eV. When a hydrogen acceptor is reduced by 1 as seen in molecule (d), then the IP decreases to 7.71 eV. These trends also correlate to local IPs at the N7 sites, and those trends are observable when looking at local ionization potential maps and seeing the decreased electron density area around N7 sites. Short range hydrogen-bonding interactions between the water and guanine leads to the re-orientation of the dipole moments that can affect the stabilization of the radical cation formed upon photoionization.

**Table 2**

Effect of specific hydrogen-bonds on the vertical gas-phase ionization potential energies of micro hydrated guanine model structures as shown in Fig. 2.

Guanine model structures	H-bond location	$IP_{ver}$ (eV) (B3LYP/6-31+G <sup>+</sup> )	Dipole moment (Debye)	$IP_{ver}$ (eV) N7 sites	$IP_{ver}$ (eV) O <sup>6</sup> sites
Guanine		7.99	6.80	8.42	9.13
(e) G+1 H <sub>2</sub> O	N1, N2	7.58	6.62	8.14	8.72
(j) G+1 H <sub>2</sub> O	O <sup>6</sup>	8.19	9.48	8.63	9.72
(f) G+2 H <sub>2</sub> O	N1, N2, O <sup>6</sup>	7.87	4.74	8.41	9.34
(g) G+2 H <sub>2</sub> O	N2, N3, O <sup>6</sup>	8.20	8.79	8.73	9.79
(h) G+2 H <sub>2</sub> O	N3, N9, N1, O <sup>6</sup>	8.01	6.20	8.38	9.40
(i) G+2 H <sub>2</sub> O	N1, N2, N3	7.64	5.34	8.25	8.94
(a) G+3 H <sub>2</sub> O	N1, N2, N3, O <sup>6</sup> , N7	8.26	8.46	9.75	10.78
(b) G+3 H <sub>2</sub> O	N1, N2, N3, N9	7.64	7.83	8.06	8.88
(c) G+3 H <sub>2</sub> O	N1, O <sup>6</sup> , N3, N9	7.93	5.32	8.35	9.44
(d) G+3 H <sub>2</sub> O	O <sup>6</sup> , N1, N2	7.71	3.81	8.34	9.31

structure (j) the water molecule hydrogen interaction with the lone pair at O<sup>6</sup> pulls electron density away from the aromatic ring making the ring slightly electrophilic. When the electron density is decreased, the IP increases because it is harder to eject an electron; here, guanine mono-hydrated at O<sup>6</sup> has an IP of 8.19 eV and water acts as a hydrogen donor. The magnitude of the dipole moment vector increases to 9.48 D, and this indicates that accumulated charge is located at larger separation distances. This effect becomes more pronounced in structure (e), where the interaction with the hydrogens at N2 and N1 pushes more electron density into the ring, decreasing the IP to 7.58 eV, making the water molecule a hydrogen bond acceptor.

This hydrogen bond donating/accepting effect becomes more evident when the number of donors and acceptors increases. The O<sup>6</sup>, N1, and N2 di-hydrated molecule, (f), has one hydrogen acceptor at the O<sup>6</sup> and two hydrogen bond donors at the N1 and N2 positions. The 2:1 ratio of donors to acceptors increases the electron density and causes the IP to decrease to 7.87 eV. Comparing molecule, (f) to the O<sup>6</sup>, N1, and N2 tri-hydrated, (d), the same 2:1 ratio is observed and the IP is decreased to 7.71 eV.

The IP for the tri-hydrated structures (a–d) is lower because the hydrogen donors discretely exchange between two water molecules, while in molecule (f) the hydrogen bonds exchange with one water molecule; both cannot bind simultaneously so the effect is not as strong. The extreme effects can be seen in molecule, (a), with H-bonds at N1, N2, N3, O<sup>6</sup>, N7 and in molecule, (b) with H-bonds N1, N2, N3, N9. In molecule (a), there are 4 hydrogen bond acceptors, two at O<sup>6</sup> and one at N7 and N3, and 2 hydrogen bond donor sites, one at N1 and one at N2. This 2:4 ratio causes the electron density of the molecule to decrease which causes the IP to increase. Also, as can be seen through molecules (b–j), electron density is localized around the N7 when electron density is pushed into the ring. When the N7 on molecule (a) is interacting with a water molecule, this localization is blocked, and the IP is pushed further up to 8.26 eV. In molecule (b), there are 3 hydrogen bond donors, at N1, N2, and N9, and only 1 hydrogen bond acceptor at N3. This 3:1 ratio pushes electron density into the ring which lowers the IP to 7.64 eV.

These results show that in micro-hydration, short range hydrogen-bonding interactions between the water and guanine leads to the re-orientation of the dipole moment that can affect the stabilization of the radical cation formed upon photoionization and lower the IP of free guanine by ~0.06 eV. This was also reported in an earlier investigation [46] that found it is very difficult in cases of micro-hydration to find a functional relation between the stabilization energy of the thymine radical cation and the re-orientation of the water dipoles.

However, within a bulk solvent environment and incorporation of the hydrated electron stabilization energy (–1.3 eV), long-range polarizations play a significant role in the stabilization energy of the guanine radical cation by 3.3 eV. Thus the effect of water molecules on the vertical IP of guanine depends on whether hydrogen-

donor or acceptor bonds are formed. But in bulk hydration, where the hydrogen bonds are averaged over a large number of water molecules, this specified hydrogen bond forming effect is eliminated.

### 3.3. Activation barriers for guanine methylation by methane diazonium ion

The reaction mechanism of guanine with methane diazonium ion, (MeN<sub>2</sub><sup>+</sup>), is an S<sub>N</sub>2 reaction characterized by the fact that guanine, the leaving group (N<sub>2</sub>) and the carbon atom of methane diazonium ion are approximately linear. In fact the angle between N7, the C atom in methane diazonium and the N atom of the leaving group is 177.6°. This angle agrees with data reported in [24]. The S<sub>N</sub>2 reaction mechanism is shown below.

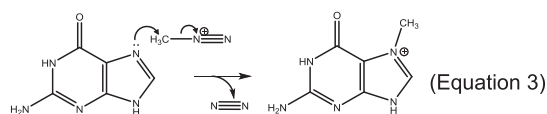
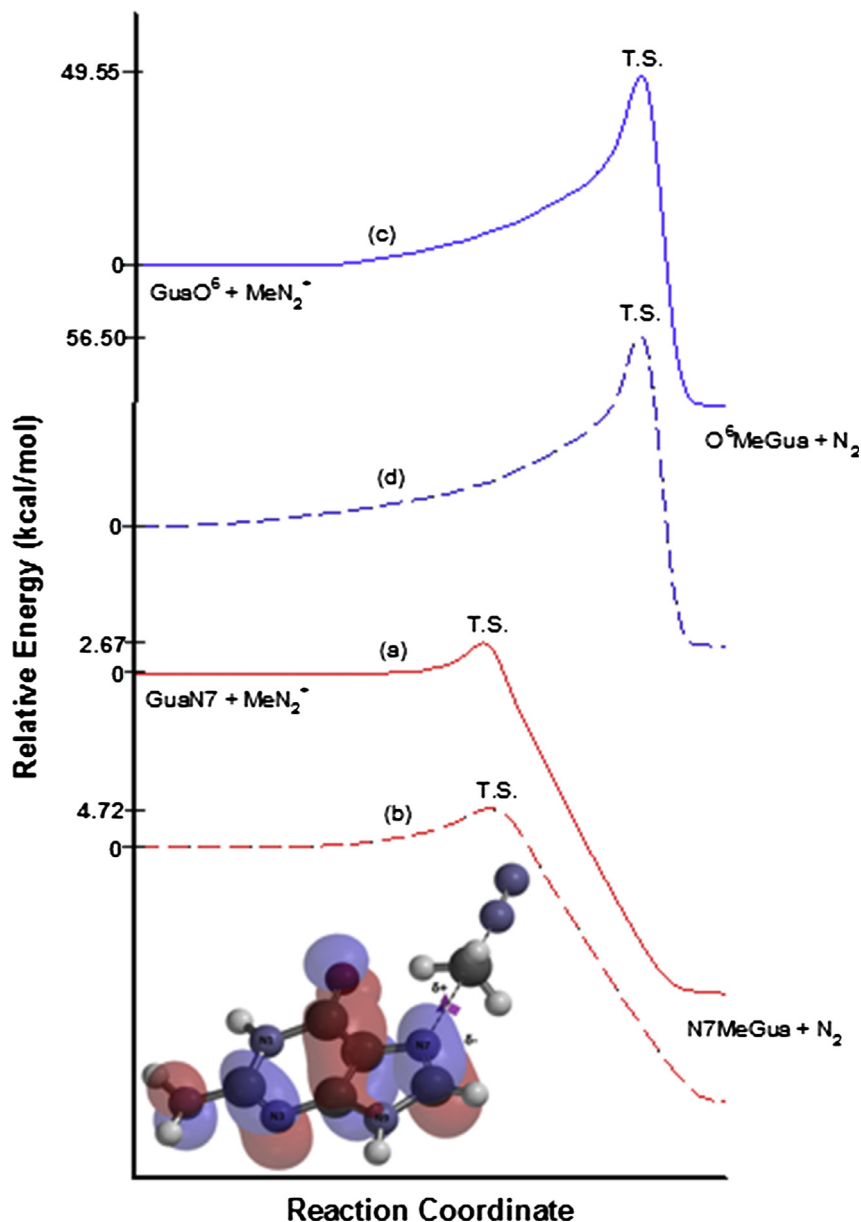


Fig. 3 shows energy profiles for the reactions of guanine at N7 and methane diazonium ion in the gas phase in curve (a) and in water in curve (b) and of guanine O<sup>6</sup> in the gas phase in curve (c) and in water in curve (d). Activation energies obtained are positive, and all reactions exhibit barriers. The activation energy values for these reactions are listed in Table 3. These activation energy values show that for reactions at the guanine N7 site the activation energy in water is higher than that in the gas-phase by 2.05 kcal mol<sup>-1</sup>, and at the O<sup>6</sup> site the activation energy was higher in solution by 6.95 kcal mol<sup>-1</sup>. For reactions at N7 site, the angle in the transition state between N7 the carbon atom of methane diazonium ion and the nitrogen atom of the ion is 176.67°, which is almost the same in both the gas-phase and in water. There is a very small, almost negligible deviation from a planar configuration, as it is supposed to be in a typical S<sub>N</sub>2 reaction.

The geometry of the transition state of the reaction at the O<sup>6</sup> site shows considerable deviation from a planar configuration. In the gas-phase the angle between O<sup>6</sup>, the carbon of the methane diazonium ion and the nitrogen atom of the leaving group is 108.34° while in water it becomes 84.56°. This deviation from a planar geometry and the distortion of the exocyclic amino group is due to steric interference that can be attributed to the repulsion between the amino group and the incoming electrophile. This repulsion increases in water. The values of the activation barriers also indicate that the N7 site of guanine is the most reactive, is in full agreement with experimentally obtained data [25].

Table 3 lists also the breaking and forming bond distances in the transition state in the gas-phase. The breaking bond distance for the N7 atom 1.538 Å and the O<sup>6</sup> atom is 1.461 Å and the bond



**Fig. 3.** Reaction profiles for methylation reactions of guanine at N7 and  $O^6$  atoms by methane diazonium ion calculated in the gas-phase employing DFT at B3LYP/6-31+G<sup>\*</sup> level and in water employing the SM8 Universal Solvation Model. The vertical axis denotes the relative energy in kcal mol<sup>-1</sup> and the horizontal axis denotes the reaction coordinate (constraint). Profiles are shown for guanine at N7, red curve (a) in the gas-phase and red curve (b) in water and for guanine at  $O^6$ , blue curve (c) in gas-phase and blue curve (d) in water. The inset shows the transition state for an in-plane attack of methane diazonium ion at the N7 atom of guanine.

**Table 3**  
Transition state geometries and activation energies of MeN<sub>2</sub><sup>+</sup> methylation of guanine.

Site	Gas phase geometry and activation energy			Aqueous activation energy $E_a$ (kcal mol <sup>-1</sup> )
	$r_{form}$ (Å)	$r_{break}$ (Å)	$E$ (kcal mol <sup>-1</sup> )	
N7	2.438	1.538	2.67	4.72
$O^6$	1.827	1.461	49.55	56.50

forming distance for the N7 atom is 2.438 Å and for the  $O^6$  atom is 1.827 Å. These distances reveal that steric interference causes the breakage of the bond to occur earlier at N7. But at  $O^6$ , the bond break occurs late and when the new bond is formed it requires more energy.

Results from both gas-phase and aqueous solution calculations show that the N7 site of guanine is more reactive than  $O^6$  and local

ionization maps reveal that the electron density at the  $O^6$  is less than that at the N7 site indicating clearly that as the IP decreases the reactivity increases. Indeed the local ionization energies for N7 is 8.42 eV and for  $O^6$  9.13 eV as listed in Table 2 and this trend is observed for all the micro-hydrated structures in Fig. 2.

In native DNA hydrogen-bonding and base-stacking interactions that occur in multiple repeating guanine sequences (G runs) have IPs that are 0.5–0.7 eV smaller than that of free guanine [47]. Applying these lower IP values the activation energies of methylation at the N7 and  $O^6$  sites are expected to change considerably.

#### 4. Conclusions

In summary the main results obtained from this investigation are the following:

1. The *syn*- conformation of gas-phase 5'-dGMP<sup>-</sup> is more stable than the *anti*-conformation by 7.57 kcal mol<sup>-1</sup> and its vertical IP is 5.03 eV and the aqueous photoionization threshold energy is 4.61 eV allowing monophotonic ionization in 266-nm (4.66 eV) laser flash photolysis experiments.
2. Gas-phase IP s are sensitive on the molecular interactions within nucleotide structure but hydration is remarkably efficient in screening these interactions.
3. In water – guanine hydrogen bonding, the water molecule can act as a hydrogen donor resulting to an increase in ionization potential or as an acceptor resulting to a decrease in the ionization potential. Local ionization potential maps provide evidence that, when electron density is pulled away from the aromatic ring, electrophilicity slightly increases and the ionization energy increases.
4. Both in the gas-phase and in aqueous solutions, the methane diazonium ion reaction with guanine follows an S<sub>N</sub>2 mechanism. The activation energy at the O<sup>6</sup> site is significantly higher than that at the N7 site. Activation energies are influenced by steric interference and local ionization energies.

### Acknowledgements

Daniel R. Eichler and Haley A. Hamann are grateful for the financial support provided by the University of Illinois at Chicago Liberal Arts and Science Undergraduate Research Initiative (LASURI) and the Department of Chemistry. GAP acknowledges stimulating discussions with Professor Donald J. Wink of the UIC Chemistry Department.

### References

- [1] J.-L. Ravanat, T. Douki, J. Cadet, J. Photochem. Photobiol., B 63 (2001) 88.
- [2] D.B. Hall, R.E. Holmlin, J.K. Barton, Nature 382 (1996) 731.
- [3] J. Cadet, E. Sage, T. Douki, Mutat. Res.-Fundament. Mole. Mech. Mutagen. 571 (2005) 3.
- [4] J. Cadet, P. Vigny, Bioorganic Photochemistry; Photochemistry and the Nucleic Acid, John Wiley & Sons, New York, 1990.
- [5] H. Fernando, G.A. Papadantonakis, N.S. Kim, P.R. LeBreton, Proc. Natl. Acad. Sci. USA 95 (1998) 5550.
- [6] C.E. Crespo-Hernández, R. Arce, Y. Ishikawa, L. Gorb, J. Leszczynski, D.M. Close, J. Phys. Chem. A 108 (2004) 6373.
- [7] D.M. Close, J. Phys. Chem. A 108 (2004) 10376.
- [8] E. Pluhařová, P. Slavíček, P. Jungwirth, Acc. Chem. Res. 48 (2015) 1209.
- [9] J.F. Ward, in: J.A. Nickoloff, M.F. Hoekstra (Eds.), DNA Damage and Repair: Volume 2: DNA Repair in Higher Eukaryotes, Humana Press, Totowa, NJ, 1998, p. 65.
- [10] A. Bacolla, N.A. Temiz, M. Yi, J. Ivancic, R.Z. Cer, D.E. Donohue, E.V. Ball, U.S. Mudunuri, G. Wang, A. Jain, N. Volfovsky, B.T. Luke, R.M. Stephens, D.N. Cooper, J.R. Collins, K.M. Vasquez, PLoS Genet 9 (2013) e1003816.
- [11] J. Lin, C. Yu, S. Peng, I. Akiyama, K. Li, L.K. Lee, P.R. LeBreton, J. Phys. Chem. 84 (1980) 1006.
- [12] X. Yang, X.B. Wang, E.R. Vorpapel, L.S. Wang, Proc. Natl. Acad. Sci. USA 101 (2004) 17588.
- [13] L. Sanche, Radiat. Phys. Chem. 128 (2016) 36.
- [14] N.S. Kim, P.R. LeBreton, J. Am. Chem. Soc. 118 (1996) 3694.
- [15] D.M. Close, K.T. Ohman, J. Phys. Chem. A 112 (2008) 11207.
- [16] L. Belau, K.R. Wilson, S.R. Leone, M. Ahmed, J. Phys. Chem. A 111 (2007) 7562.
- [17] K. Okamoto, S. Toyokuni, K. Uchida, O. Ogawa, J. Takenawa, Y. Kakehi, H. Kinoshita, Y. Hattori-Nakakuki, H. Hiai, O. Yoshida, Int. J. Cancer 58 (1994) 825.
- [18] S. Lagadu, M. Lechevrel, F. Sichel, J. Breton, D. Pottier, R. Couderc, F. Moussa, V. Prevost, J. Exper. Clin. Cancer Res. 29 (2010) 1.
- [19] B. Singer, D. Grunberger, Molecular Biology of Mutagens and Carcinogens, Plenum Press, 1983.
- [20] W. Lijinsky, Chemistry and biology of N-nitroso compounds, Cambridge University Press, 1992.
- [21] Y. Kou, M.-C. Koag, S. Lee, J. Am. Chem. Soc. 137 (2015) 14067.
- [22] G.P. Ford, J.D. Scribner, J. Am. Chem. Soc. 105 (1983) 349.
- [23] G.P. Ford, J.D. Scribner, Chem. Res. Toxicol. 3 (1990) 219.
- [24] N. Nakayama, S. Tanaka, O. Kikuchi, J. Theor. Biol. 215 (2002) 13.
- [25] K.S. Ekanayake, P.R. LeBreton, J. Comput. Chem. 27 (2005) 277.
- [26] R. Chakraborty, D. Ghosh, Phys. Chem. Chem. Phys. 18 (2016) 6526.
- [27] C.E. Crespo-Hernández, D.M. Close, L. Gorb, J. Leszczynski, J. Phys. Chem. B 111 (2007) 5386.
- [28] C.A. Schroeder, E. Pluhařová, R. Seidel, W.P. Schroeder, M. Faubel, P. Slavíček, B. Winter, P. Jungwirth, S.E. Bradforth, J. Am. Chem. Soc. 137 (2015) 201.
- [29] A. Kumar, A. Adhikary, L. Shamoun, M.D. Sevilla, J. Phys. Chem. B 120 (2016) 2115.
- [30] A.V. Marenich, R.M. Olson, C.P. Kelly, C.J. Cramer, D.G. Truhlar, J. Chem. Theory Comput. 3 (2007) 2011.
- [31] I. Wavefunction, Spartan '14 Parallel Suite, Irvine, CA, 2014.
- [32] D. Grand, A. Bernas, E. Amouyal, Chem. Phys. 44 (1979) 73.
- [33] E. Amouyal, A. Bernas, D. Grand, Photochem. Photobiol. 29 (1979) 7.
- [34] J.E. Bartmess, J. Phys. Chem. 98 (1994) 6420.
- [35] V.V. Zakjevskii, S.J. King, O. Dolgounitcheva, V.G. Zakrzewski, J.V. Ortiz, J. Am. Chem. Soc. 128 (2006) 13350.
- [36] M. Rubio, D. Roca-Sanjuán, L. Serrano-Andrés, M. Merchán, J. Phys. Chem. B 113 (2009) 2451.
- [37] A.S. Chatterley, A.S. Johns, V.G. Stavros, J.R.R. Verlet, J. Phys. Chem. A 117 (2013) 5299.
- [38] C.E. Crespo-Hernández, S. Flores, C. Torres, I. Negrón-Encarnación, R. Arce, Photochem. Photobiol. 71 (2000) 534.
- [39] G.A. Papadantonakis, K.L. Stevenson, P.R. LeBreton, Chem. Phys. Lett. 346 (2001) 97.
- [40] C.E. Crespo-Hernández, R. Arce, J. Phys. Chem. B 107 (2003) 1062.
- [41] A. Hocquet, N. Leulliot, M. Ghomi, J. Phys. Chem. B 104 (2000) 4560.
- [42] N. Foloppe, B. Hartmann, L. Nilsson, A.D. MacKerell, Biophys. J. 82 (2002) 1554.
- [43] G.A. Papadantonakis, R. Tranter, K. Brezinsky, Y. Yang, R.B. van Breemen, P.R. LeBreton, J. Phys. Chem. B 106 (2002) 7704.
- [44] H.S. Kim, M. Yu, Q. Jiang, P.R. LeBreton, J. Am. Chem. Soc. 115 (1993) 6169.
- [45] N.S. Kim, Q. Jiang, P.R. LeBreton, Int. J. Quantum Chem. 60 (1996) 1735.
- [46] D.M. Close, C.E. Crespo-Hernandez, L. Gorb, J. Leszczynski, J. Phys. Chem. A 110 (2006) 7485.
- [47] Q. Zhu, P.R. LeBreton, J. Am. Chem. Soc. 122 (2000) 12824.